

SOME THEORETICAL INVESTIGATIONS ON DIELECTRIC ROD WAVEGUIDE

BY V. SUBRAHMANIAM

(Department of Electrical Communication Engineering, Indian Institute of Science, Bangalore-12)

Received on April 25, 1962

ABSTRACT

The propagation characteristics of the HE_{11} -mode launched on a circular cylindrical dielectric rod wave guide, such as the radial propagation constant, the axial propagation constant and the guide wavelength at 3.2 cms. wavelength have been studied theoretically as a function of the diameter and the dielectric constant of the rod. The electric field distributions and the power flow as a function of the diameter and the dielectric constant of the rod have also been calculated for both inside and outside the rod.

INTRODUCTION

Several authors¹⁻¹⁵ have investigated the propagation characteristics of electromagnetic waves launched on dielectric rods, planes, conducting plane with dielectric coating, corrugated plane and cylindrical conducting structures etc. The object of this paper is to present a theoretical study of the propagation characteristics of the HE_{11} -mode launched on a circular cylindrical dielectric rod, with particular reference to the variation of

(i) the radial propagation constants k_1 and k_2 inside and outside the dielectric rod respectively as a function of the diameter (d) and the relative dielectric constant ($\bar{\epsilon}_1$) of the rod at a wavelength of $\lambda_0 = 3.2$ cms.

(ii) the axial propagation constant γ as a function of d and $\bar{\epsilon}_1$

(iii) the guide wavelength λ_g as a function of d and $\bar{\epsilon}_1$.

The electric field distributions (E_ρ, E_ϕ, E_z) inside and outside the rod of dielectric constant $\bar{\epsilon}_1 = 2.6$ and of different diameters have also been calculated. The power flow inside the rod as a percentage of the total power flow has also been calculated as a function of d and $\bar{\epsilon}_1$ and some of the results are presented graphically.

Field Components: The field components inside and outside the circular cylindrical dielectric guide of radius r are the following¹⁶ :—
Inside the dielectric, $\rho \leq r$ (Medium 1)

$$E_{\rho 1} = -B \left[\frac{1}{\rho} J_1(k_1 \rho) + \frac{b}{B} \cdot \frac{\gamma_1 k_1}{i \omega \epsilon_1} J_1'(k_1 \rho) \right] \sin \phi \cdot e^{-\gamma_1 z}$$

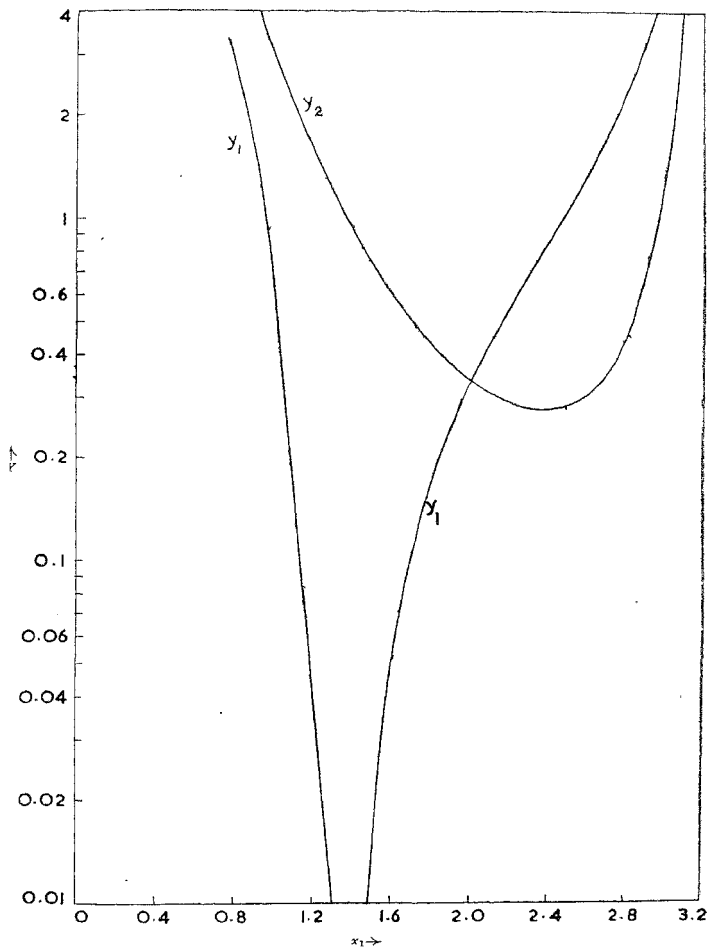


FIG. 1

Graphical solution of the characteristic equation [7] for $d/\lambda_0=0.8$, $\epsilon_1=2.6$ and $\lambda_0=3.2$ cms.

$$\begin{aligned}
E_{\phi 1} &= -B \left[k_1 J_1'(k_1 \rho) + \frac{b}{B} \cdot \frac{1}{\rho} \cdot \frac{\gamma_1}{i \omega \epsilon_1} J_1(k_1 \rho) \right] \cos \phi \cdot e^{-\gamma_1 z} \\
E_{z 1} &= B \left[\frac{b}{B} \cdot \frac{k_1^2}{i \omega \epsilon_1} J_1(k_1 \rho) \right] \sin \phi \cdot e^{-\gamma_1 z} \\
H_{\rho 1} &= B \left[\frac{\gamma_1 k_1}{i \omega \mu_1} J_1'(k_1 \rho) + \frac{b}{B} \cdot \frac{1}{\rho} J_1(k_1 \rho) \right] \cos \phi \cdot e^{-\gamma_1 z} \\
H_{\phi 1} &= -B \left[\frac{1}{\rho} \cdot \frac{\gamma_1}{i \omega \mu_1} J_1(k_1 \rho) + \frac{b}{B} k_1 J_1'(k_1 \rho) \right] \sin \phi \cdot e^{-\gamma_1 z} \\
H_{z 1} &= -B \left[\frac{k_1^2}{i \omega \mu_1} J_1(k_1 \rho) \right] \cos \phi \cdot e^{-\gamma_1 z} \tag{1}
\end{aligned}$$

Outside the dielectric, $\rho \geq r$ (Medium 2)

$$\begin{aligned}
E_{\rho 2} &= -C \left[\frac{1}{\rho} H_1^{(1)}(k_2 \rho) + \frac{c}{C} \frac{\gamma_2 k_2}{i \omega \epsilon_2} H_1^{(1)'}(k_2 \rho) \right] \sin \phi \cdot e^{-\gamma_2 z} \\
E_{\phi 2} &= -C \left[k_2 H_1^{(1)'}(k_2 \rho) + \frac{c}{C} \frac{1}{\rho} \frac{\gamma_2}{i \omega \epsilon_2} H_1^{(1)}(k_2 \rho) \right] \cos \phi \cdot e^{-\gamma_2 z} \\
E_{z 2} &= C \left[\frac{c}{C} \frac{k_2^2}{i \omega \epsilon_2} H_1^{(1)}(k_2 \rho) \right] \sin \phi \cdot e^{-\gamma_2 z} \\
H_{\rho 2} &= C \left[\frac{\gamma_2 k_2}{i \omega \mu_2} H_1^{(1)'}(k_2 \rho) + \frac{c}{C} \frac{1}{\rho} H_1^{(1)}(k_2 \rho) \right] \cos \phi \cdot e^{-\gamma_2 z} \\
H_{\phi 2} &= -C \left[\frac{1}{\rho} \frac{\gamma_2}{i \omega \mu_2} H_1^{(1)}(k_2 \rho) + \frac{c}{C} k_2 H_1^{(1)'}(k_2 \rho) \right] \sin \phi \cdot e^{-\gamma_2 z} \\
H_{z 2} &= -C \left[\frac{k_2^2}{i \omega \mu_2} H_1^{(1)}(k_2 \rho) \right] \cos \phi \cdot e^{-\gamma_2 z} \tag{2}
\end{aligned}$$

where k_1 and k_2 are the radial propagation constants, γ_1 and γ_2 are the axial constants, μ_1 and μ_2 are the permeabilities of media 1 and 2 respectively, ϵ_1 and ϵ_2 are the dielectric constants of the two media, b, c, B and C are constants to be determined by the boundary conditions. The Bessel function $J_1(x)$ and the Hankel function $H_1^{(1)}(x)$ have been used for the field components inside

and outside the guide in order to ensure the regularity of the field on the axis of the guide and to satisfy the condition at infinity respectively. The time variation $\exp(j\omega t)$ has been omitted from eqn. [2] for convenience.

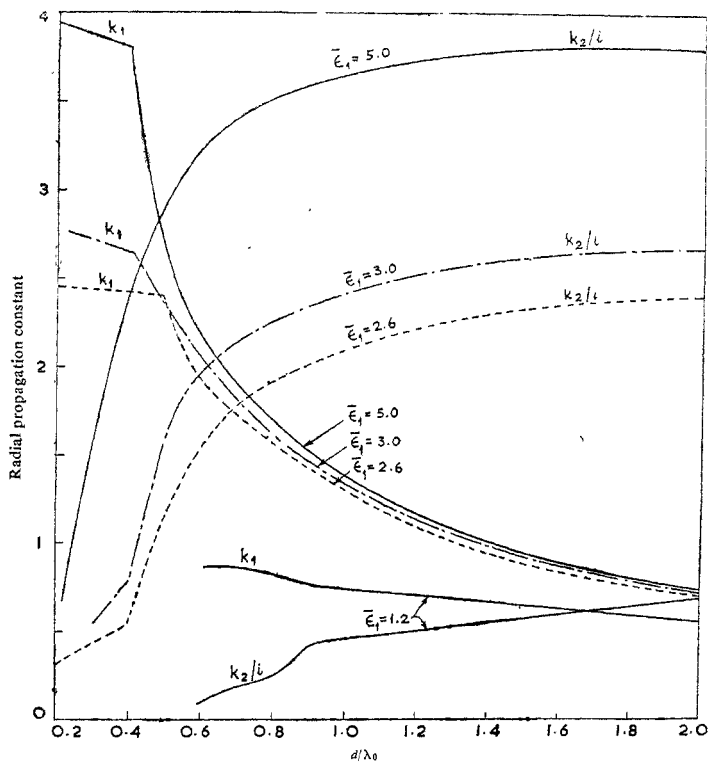


FIG. II

Variation of the radial propagation constants k_1 and k_2 with d/λ_0 ($\lambda_0 = 3.2$ cms)
(As k_2 is imaginary— $i k_2$ has been plotted)

Boundary condition: The following boundary conditions at $\rho = r$ are to be satisfied:—

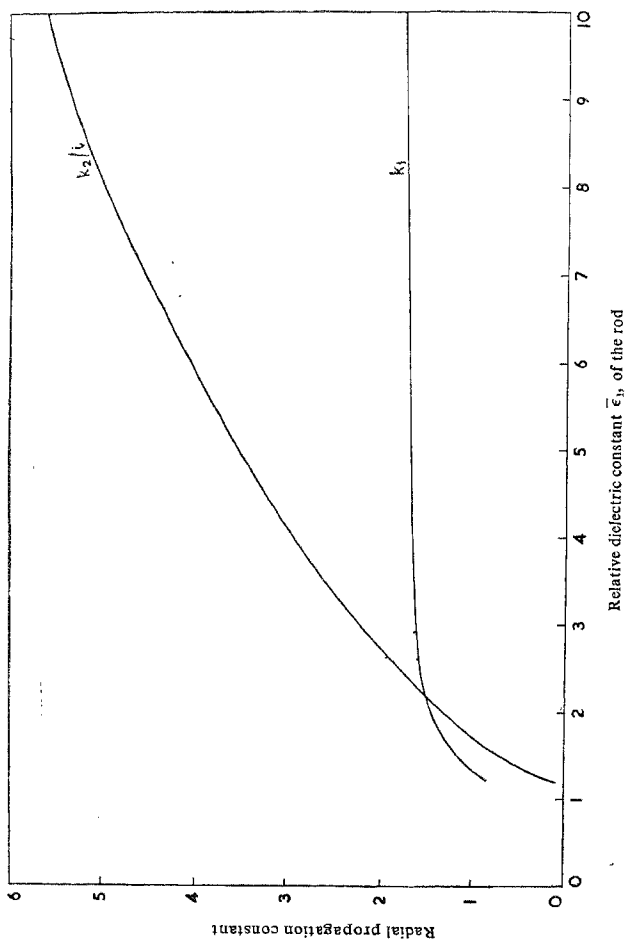


FIG. III

Variation of the radial propagation constant k_1 and k_2 with $\bar{\epsilon}_1$ ($d/\lambda_0=0.8$, $\lambda_0=3.2$ cms.),

$$E_{z1} = E_{z2}, E_{\phi 1} = E_{\phi 2} \quad (a)$$

$$H_{z1} = H_{z2}, H_{\phi 1} = H_{\phi 2} \quad (b) \quad [3]$$

It is also necessary, for a single hybrid mode to exist, that

$$\gamma_1 = \gamma_2 = \gamma = \sqrt{(k_1^2 - \omega^2 \mu_1 \epsilon_1)} = \sqrt{(k_2^2 - \omega^2 \mu_2 \epsilon_2)} \quad [4]$$

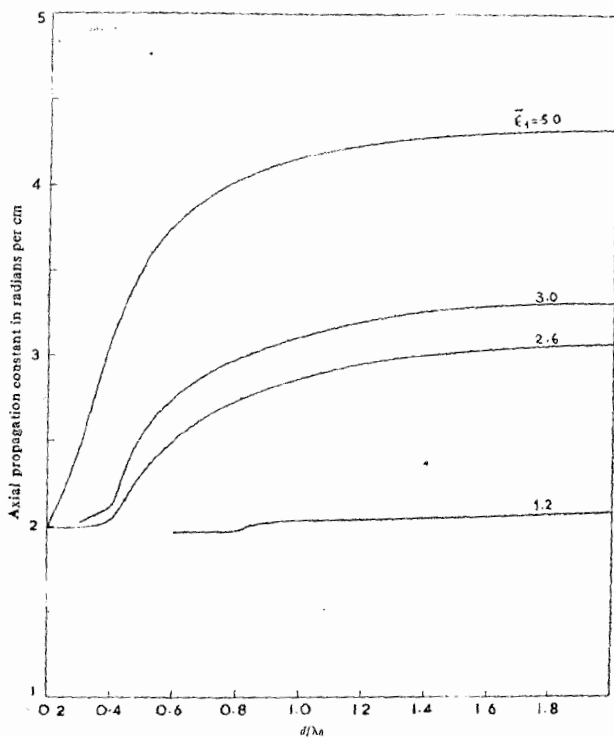


FIG. IV

Variation of the axial propagation constant γ , with d/λ_0 for $\lambda_0 = 3.2$ cms,

Characteristic Equation: From the equations [1], [2] and [3], the following equations are obtained:—

$$B k_1 J_1'(k_1 r) + \frac{b}{r} \cdot \frac{\gamma}{i \omega \epsilon_1} J_1(k_1 r) = C k_2 H_1^{(1)'}(k_2 r) + \frac{c}{r} \cdot \frac{\gamma}{i \omega \epsilon_2} H_1^{(1)'}(k_2 r)$$

$$b \frac{k_1^2}{i \omega \epsilon_1} J_1(k_1 r) = c \frac{k_2^2}{i \omega \epsilon_2} H_1^{(1)}(k_2 r) \quad [5]$$

$$\frac{B}{r} \cdot \frac{\gamma}{i \omega \mu_1} J_1(k_1 r) + b k_1 J_1'(k_1 r) = \frac{C}{r} \cdot \frac{\gamma}{i \omega \mu_2} H_1^{(1)}(k_2 r) + C k_2 H_1^{(1)'}(k_2 r)$$

$$B \frac{k_1^2}{i \omega \mu_1} J_1(k_1 r) = C \frac{k_2^2}{i \omega \mu_2} H_1^{(1)}(k_2 r) \quad [6]$$

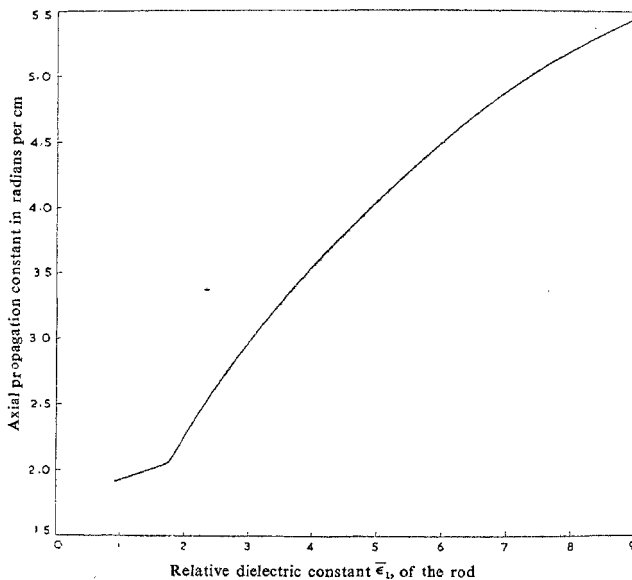


FIG. 5

Variation of the axial propagation constant γ , with $\bar{\epsilon}_1$ for $d/\lambda_0=0.8$ and $\lambda_0=3.2$ cms.

The equations [5] and [6] have a nontrivial solution if the determinant of the coefficients of the constants b , B , c and C vanishes. Expansion of this determinant leads to the following characteristic transcendental equation.

$$\left[\frac{1}{x_1} \cdot \frac{J_1'(x_1)}{J_1(x_1)} - \frac{1}{x_2} \cdot \frac{H_1^{(1)'}(x_2)}{H_1^{(1)}(x_2)} \right] \cdot \left[\frac{\bar{\epsilon}_1}{x_1} \cdot \frac{J_1'(x_1)}{J_1(x_1)} - \frac{1}{x_2} \cdot \frac{H_1^{(1)'}(x_2)}{H_1^{(1)}(x_2)} \right] \\ = \frac{(x_1^2 - x_2^2)(x_1^2 - \bar{\epsilon}_1 x_2^2)}{x_1^4 x_2^4} \quad [7]$$

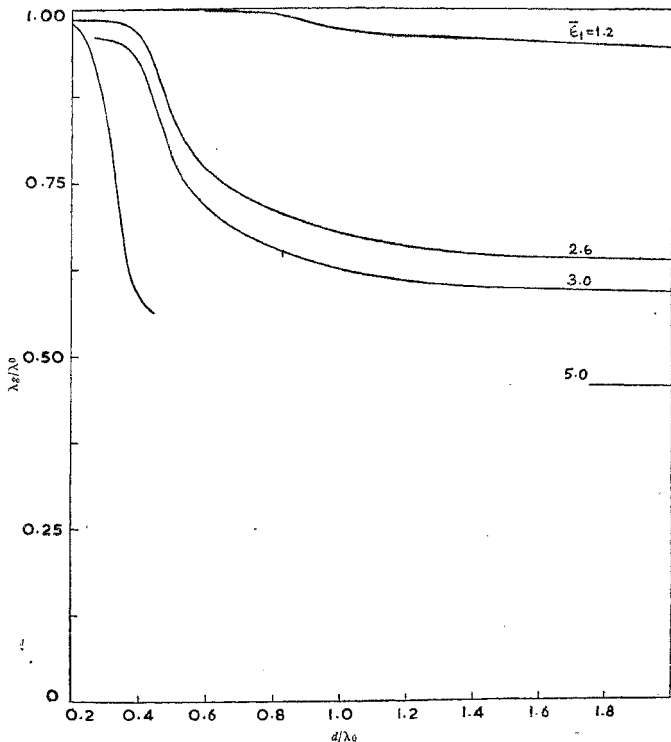


FIG. VI

Variation of λ_g/λ_0 with d/λ_0 for the HE_{11} -mode ($\lambda_0=3.2$ cms).

where $x_1 = k_1 r$; $x_2 = k_2 r$ [8]

and x_1 and x_2 are also related by the following equation:—

$$x_1^2 + \left(\frac{x_2}{i}\right)^2 = \left(\frac{\pi d}{\lambda_0}\right)^2 (\bar{\epsilon}_1 - 1) \quad [9]$$

Solution of the Characteristic equation: The characteristic equation [7] has been solved in the following way:—

Let

$$Y_1 = \left[\frac{1}{x_1} \frac{J_1'(x_1)}{J_1(x_1)} - \frac{1}{x_2} \frac{H_1^{(1)'}(x_2)}{H_1^{(1)}(x_2)} \right] \cdot \left[\frac{\bar{\epsilon}_1}{x_1} \frac{J_1'(x_1)}{J_1(x_1)} - \frac{1}{x_2} \frac{H_1^{(1)'}(x_2)}{H_1^{(1)}(x_2)} \right] \quad [10]$$

$$\text{and } Y_2 = \frac{(x_1^2 - x_2^2)(x_1^2 - \bar{\epsilon}_1 x_2^2)}{x_1^2 x_2^2} \quad [11]$$

Y_1 and Y_2 are expressed as a function of x_1 only with the help of the equation [9]. The values of (x_2/i) are calculated corresponding to some arbitrary values of x_1 for a particular value of d/λ_0 and $\bar{\epsilon}_1$. Y_1 and Y_2 are then plotted as a function of x_1 . The intersection of Y_1 and Y_2 gives the root x_1 and hence x_2 of the equation [7]. The procedure is repeated for different values of d/λ_0 and $\bar{\epsilon}_1$. As an illustration the graphical solution for $d/\lambda_0 = 0.8$ and $\bar{\epsilon}_1 = 2.6$ is presented in Fig. I.

Radial and Axial propagation constants:—The radial propagation constants k_1 and k_2 are calculated from equation [8]. They have been plotted as a function of d/λ_0 for $\bar{\epsilon}_1 = 2.6$ in Fig. II, and a function of $\bar{\epsilon}_1$ for $d/\lambda_0 = 0.8$ in Fig. III. The axial propagation constant γ is calculated from equation [4] and its variation with d/λ_0 and $\bar{\epsilon}_1$ is shown in Fig. IV and V respectively. It is observed that k_1 decreases and k_2 and γ increase with increasing values of d and $\bar{\epsilon}_1$ and this gives rise to the reduction of the radial field spread.

Guide Wavelength: The guide wavelength λ_g is obtained from equations [4] and [9] and is as follows:—

$$\frac{\lambda_g}{\lambda_0} = \left[\bar{\epsilon}_1 - \left(\frac{x_1}{\pi d/\lambda_0} \right)^2 \right]^{-1} \quad [12]$$

The values of λ_g/λ_0 as computed from the above expression are plotted in Fig. VI as a function of d/λ_0 (from 0.2 to 1.8) and $\bar{\epsilon}_1 = 2.6$ and as a function of $\bar{\epsilon}_1$ (from 1 to 10) for $d/\lambda_0 = 0.8$ in Fig. VII. It is observed that λ_g decreases

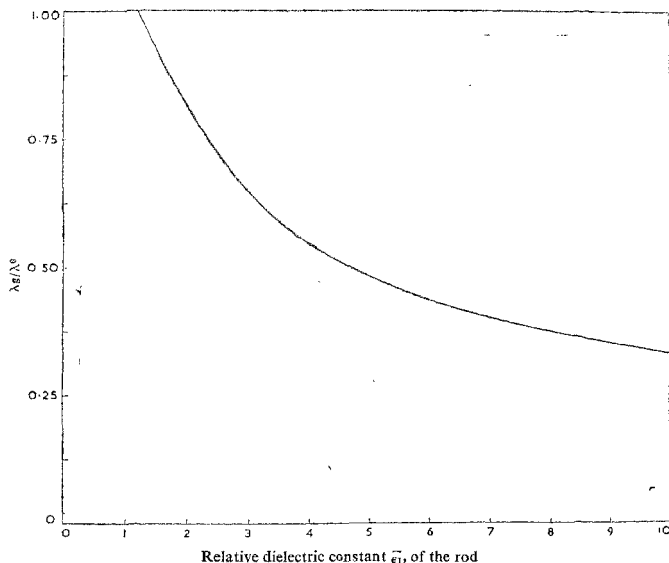


FIG. VII

Variation of λ_g/λ_0 with $\bar{\epsilon}_1$ for the HE_{11} -mode ($d/\lambda_0 = 0.8$, $\lambda_0 = 3.2$ cms).

with an increase in $\bar{\epsilon}_1$ as is expected. The decrease of λ_g with an increase in the diameter of the rod may be due to the increase of γ , as an increase in γ ($=i\beta$) for a lossless waveguide reduces the phase velocity of the propagating wave. The reduction in phase velocity is responsible for the decrease of λ_g with increase of d .

Field Configuration:—The constants b , B , c and C as obtained from equations [5] and [6] are given by the following expressions:—

$$\frac{b}{B} = \frac{\gamma \epsilon_1}{i \omega \mu_1} \cdot \frac{x_1^2 - x_2^2}{x_1^2 x_2^2} \cdot \left[\frac{\epsilon_1 J_1'(x_1)}{x_1 J_1(x_1)} - \frac{\epsilon_2 H_1^{(1)'}(x_2)}{x_2 H_1^{(1)}(x_2)} \right]^{-1} \quad [13]$$

$$\frac{c}{B} = \frac{x_1^2}{x_2^2} \cdot \frac{\mu_2}{\mu_1} \cdot \frac{J_1(x_1)}{H_1^{(1)}(x_2)} \quad [14]$$

$$\frac{c}{b} = \frac{x_1^2}{x_2^2} \cdot \frac{\epsilon_2}{\epsilon_1} \cdot \frac{J_1(x_1)}{H_1^{(1)}(x_2)} \quad [15]$$

$$\text{and} \quad \frac{c}{C} = \frac{\gamma \epsilon_2}{i \omega \mu_2} \cdot \frac{x_1^2 - x_2^2}{x_1^2 x_2^2} \cdot \left[\frac{\epsilon_1}{x_1} \cdot \frac{J_1'(x_1)}{J_1(x_1)} - \frac{\epsilon_2}{x_2} \cdot \frac{H_1^{(1)'}(x_2)}{H_1^{(1)}(x_2)} \right]^{-1} \quad [16]$$

The constants are evaluated for different values of d/λ_0 and $\bar{\epsilon}_1$. The electric field components (E_ρ , E_ϕ and E_z) inside and outside the rod are then evaluated for different values of d/λ_0 and some of the results are presented graphically in Figures VIII, IX and X. The values of the field components have been normalized

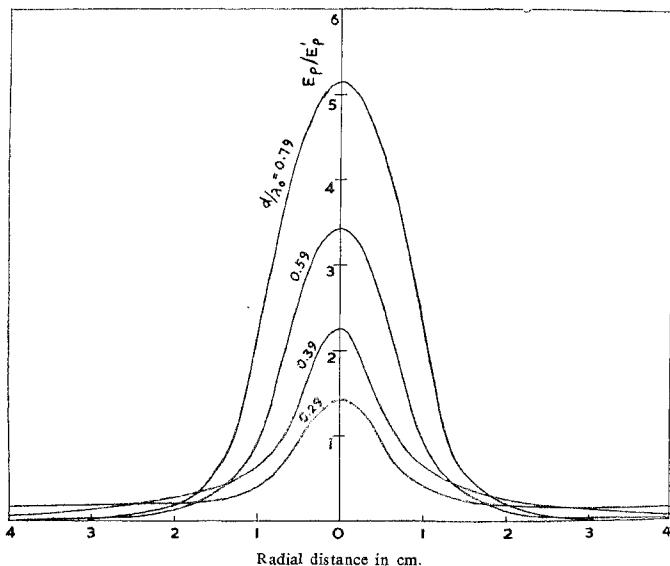


FIG. VIII

Variation of the radial component, E_ρ of the electric field with the radial distance, ρ .
($\bar{\epsilon}_1 = 2.6$, $\lambda_0 = 3.2$ cms).

(E_ρ has been normalized with respect to its value E_ρ' on the surface of the rod)

with respect to their values at the surface of the rod. The decrease of k_1 and the increase of k_2 and γ with the increase of d are responsible for the reduction of the field spread in the radial direction.

Power Flow: The power flow, w_i , along the z-direction inside the rod per unit area is given by

$$w_i = \frac{1}{2} \left[E_{\rho 1} H_{\phi 1}^* - E_{\phi 1} H_{\rho 1}^* \right] \quad [17]$$

The power flow inside the rod is

$$W_i = \frac{1}{2} \int_{\rho=0}^r \int_{\phi=0}^{2\pi} \left[E_{\rho 1} H_{\phi 1}^* - E_{\phi 1} H_{\rho 1}^* \right] \rho \, d\rho \, d\phi \quad [18]$$

which yields

$$\begin{aligned} W_i = & B^2 \left[\frac{b}{B} \pi k_1 \left(1 - \frac{\gamma^2}{\omega^2 \mu_1 \epsilon_1} \right) \int_{\rho=0}^r J_0(k_1 \rho) J_1(k_1 \rho) \, d\rho \right. \\ & - \frac{\pi \gamma k_1}{i \omega} \left(\frac{1}{\mu_1} + \frac{b^2}{B^2} \cdot \frac{1}{\epsilon_1} \right) \int_{\rho=0}^r J_0(k_1 \rho) J_1(k_1 \rho) \, d\rho \\ & + \frac{\pi \gamma}{i \omega} \left(\frac{1}{\mu_1} + \frac{b^2}{B^2} \cdot \frac{1}{\epsilon_1} \right) \int_{\rho=0}^r \frac{1}{\rho} [J_1(k_1 \rho)]^2 \, d\rho \\ & - \frac{b}{B} \pi \left(1 - \frac{\gamma^2}{\omega^2 \mu_1 \epsilon_1} \right) \int_{\rho=0}^r \frac{1}{\rho} [J_1(k_1 \rho)]^2 \, d\rho \\ & \left. + \frac{\pi \gamma k_1^2}{2 i \omega} \left(\frac{1}{\mu_1} + \frac{b^2}{B^2} \cdot \frac{1}{\epsilon_1} \right) \int_{\rho=0}^r \rho [J_0(k_1 \rho)]^2 \, d\rho \right] \quad [19] \end{aligned}$$

The power flow outside the rod is

$$W_0 = \frac{1}{2} \int_{\rho=r}^{\infty} \int_{\phi=0}^{2\pi} [E_{\rho 2} H_{\phi 2}^* - E_{\phi 2} H_{\rho 2}^*] \rho \, d\rho \, d\phi \quad [20]$$

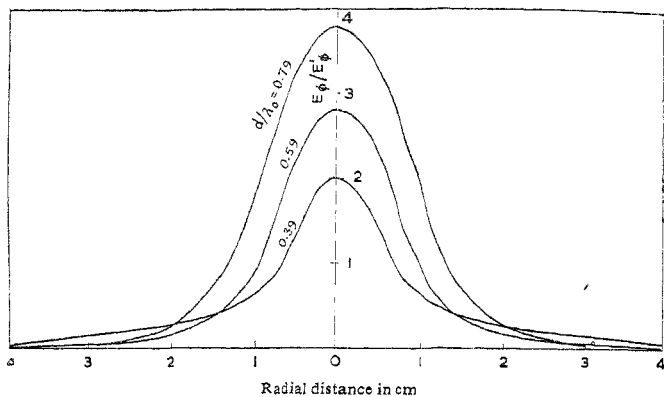


FIG. IX

Variation of the azimuthal component E_ϕ , of the electric field with the radial distance, ρ .
 ($\epsilon_1=2.6$, $\lambda_0=3.2$ cms).
 (E_ϕ has been normalized with respect to its value E_ϕ^0 on the surface of the rod).

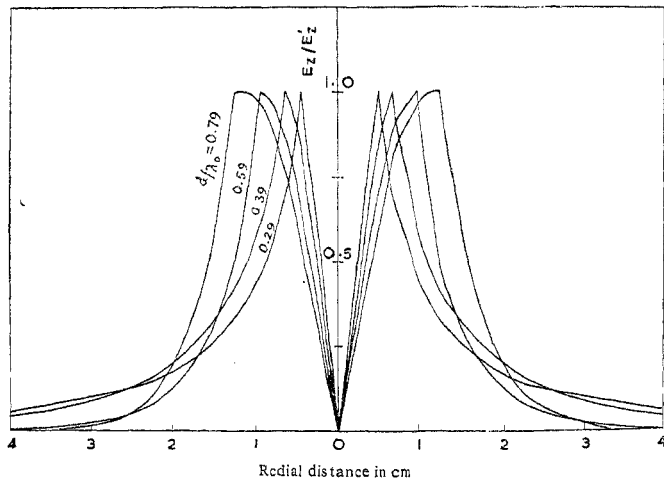


FIG. X

Variation of the axial component, E_z , of the electric field with radial distance ρ .
 ($\epsilon_1=2.6$, $\lambda_0=3.2$ cms).

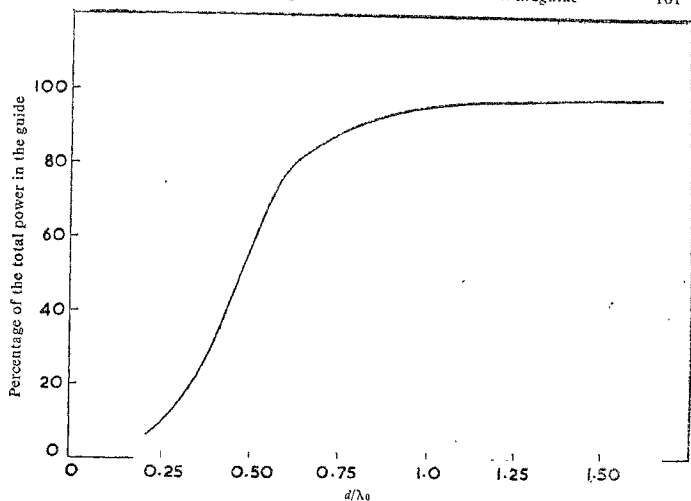


FIG. XI

Percentage power flow inside the waveguide vs. d/λ_0 ($\bar{\epsilon}_1=2.6$, $\lambda_0=3.2$ cms).

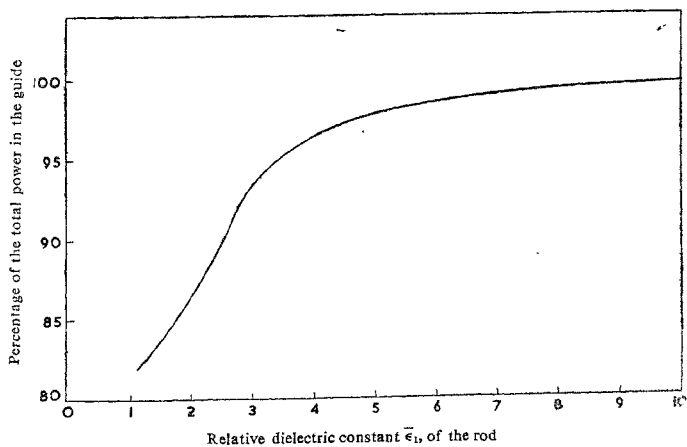


FIG. XII

Percentage power flow inside the waveguide vs. $\bar{\epsilon}_1$ ($d/\lambda_0=0.8$, $\lambda_0=3.2$ cms).

which yields

$$\begin{aligned}
 W_0 = C^2 & \left[\frac{c}{C} \pi k_2 \left(1 - \frac{\gamma^2}{\omega^2 \mu_2 \epsilon_2} \right) \int_{\rho=r}^{\infty} H_0^{(1)}(k_2 \rho) H_1^{(1)}(k_2 \rho) d\rho \right. \\
 & - \frac{\pi \gamma k_2}{i \omega} \left(\frac{1}{\mu_2} + \frac{c^2}{C^2} \cdot \frac{1}{\epsilon_2} \right) \int_{\rho=r}^{\infty} H_0^{(1)}(k_2 \rho) H_1^{(1)}(k_2 \rho) d\rho \\
 & + \frac{\pi \gamma}{i \omega} \left(\frac{1}{\mu_2} + \frac{c^2}{C^2} \cdot \frac{1}{\epsilon_2} \right) \int_{\rho=r}^{\infty} \frac{1}{\rho} [H_1^{(1)}(k_2 \rho)]^2 d\rho \\
 & - \frac{c}{C} \pi \left(1 - \frac{\gamma^2}{\omega^2 \mu_2 \epsilon_2} \right) \int_{\rho=r}^{\infty} \frac{1}{\rho} [H_1^{(1)}(k_2 \rho)]^2 d\rho \\
 & \left. + \frac{\pi \gamma k_2}{2 i \omega} \left(\frac{1}{\mu_2} + \frac{c^2}{C^2} \cdot \frac{1}{\epsilon_2} \right) \int_{\rho=r}^{\infty} \rho [H_0^{(1)}(k_2 \rho)]^2 d\rho \right] \quad [21]
 \end{aligned}$$

The expressions for W_i and W_0 are evaluated by numerical integration for different values of d/λ_0 and $\bar{\epsilon}_1$. From these values of W_i and W_0 , W_i is expressed as a percentage of the total power W_T flowing in the rod and some of the results are presented in Fig. XI and XII.

$$\frac{W_i}{W_T} = \frac{(W_i/W_0)}{1 + (W_i/W_0)}$$

It is observed that the power flow is more and more concentrated inside the guide as the dielectric constant or the diameter of the rod is increased. This is justified by the fact that the radial field spread is reduced as d or $\bar{\epsilon}_1$ increases.

ACKNOWLEDGEMENT

The author expresses his thanks to Prof. S. K. Chatterjee for suggesting the problem and for guidance and to Dr. (Mrs.) R. Chatterjee for helpful discussions. The author is grateful to Prof. S. V. C. Aiyar for the encouragement and the facilities provided during the course of the work. The author also expresses his gratitude to the University Grants Commission for the award of a Fellowship; to the Secretary, Birla Educational Trust and to Dr. S. M. Mitra, Principal, Birla College, Pilani for granting study leave.

REFERENCES

1. J. Zenneck *Ann. Phys.*, 1907, **23**, 846.
2. Hondros and Debye *Ibid*, 1910, **32**, 465.
3. Carson, J. R., Mead, S. P. and Schelkunoff, S. A. *Bell System Tech. J.*, 1936, **15**, 310.
4. Southworth, G. C. *Ibid*, 1936, **15**, 284.
5. Muller, G. E. and Tyrrel, W. A. *Ibid*, 1947, **26**, 837.
6. Whitmel, R. M. *Proc. I.R.E.*, Sept. 1948, **36**, 1105.
7. Elsasser, W. M. *J. Appl. Phys.*, 1949, **20**, 1193.
8. Chandler, C. H. *Ibid*, Dec. 1949, **20**, 1189.
9. Attwood, S. S. *Ibid*, April 1954, **22**, 504.
10. Weiss, M. T. and Gyorgy, E. M. *I.R.E., Trans.*, Sept. 1954, *PGMTT-2*, 238.
11. Barone, S. *Polytech. Inst. Brooklyn*, Nov. 1956, MRI. Res. Rep. R. 532.
12. Du Hamel, R. H. and Duncan, J. W. *I. R. E., Trans.*, July 1958, *PGMTT-6*, 277.
13. Duncan, J. W. *Ibid*, April 1959, *PGMTT-7*, 257.
14. Clarricoats, P. J. B. *Proc. I. E. E.*, March 1961, **13**, Monograph, 409 E, 108 C.
15. ————— *Ibid*, March 1961, **13**, Monograph, 410 R, 108 C.
16. Halliday, D. F. and Kiely, D G. *J. I. E. E.* 1947, **94**, Part III A, 610.